Separation, detection and characterisation of nanomaterials in municipal wastewaters using hydrodynamic chromatography coupled to ICPMS and single particle ICPMS

Kim Proulx [A], Madjid Hadioui [A] and Kevin J. Wilkinson [A,*]

[A]Department of Chemistry, Biophysical Environmental Chemistry group, University of Montreal, C.P. 6128, succursale Centre-ville, Montreal (QC), Canada H3C 3J7

*kj.wilkinson@umontreal.ca; ORCID: 0000-0002-7182-3624

Accepted for publication in *Anal. Bioanal. Chem.* 2016, 408: 5147-5155. DOI: 10.1007/s00216-016-9451-x

Abstract

Engineered nanoparticles (ENP) are increasingly being incorporated into consumer products and reaching the environment at a growing rate. Unfortunately, few analytical techniques are available that allow the detection of ENP in complex environmental matrices. The major limitations with existing techniques are their relatively high detection limits and their inability to distinguish ENP from other chemical forms (e.g. ions, dissolved) or from natural colloids. Of the matrices that are considered to be a priority for method development, ENP are predicted to be found at relatively high concentrations in wastewaters and wastewater biosolids. In this paper, we demonstrate the capability of hydrodynamic chromatography (HDC) coupled to inductively coupled plasma mass spectrometry (ICPMS), in its classical and single particle modes (SP ICPMS), to identify ENP in wastewater influents and effluents. The paper first focuses on the detection of standard silver nanoparticles (Ag NP) and their mixtures, showing that significant dissolution of the Ag NP was likely to occur. For the Ag NP, detection limits of 0.03 µg L^{-1} were found for the HDC ICPMS whereas 0.1 µg L^{-1} was determined for the HDC SP ICPMS (based on results for the 80 nm Ag NP). In the second part of the paper, HDC ICPMS and HDC SP ICPMS was performed on some unspiked natural samples (wastewaters, river water). While nanosilver was below detection limits, it was possible to identify some (likely natural) Cu nanoparticles using the developed separation technology.

Keywords

Nanosilver, nanoparticles, hydrodynamic chromatography, single particle ICPMS, wastewaters

Introduction

Engineered nanoparticles (ENP) are products with at least one dimension in the 1-100 nm size range. Their enhanced reactivity with respect to bulk materials, makes them interesting for a number of applications [1]. Indeed, ENP such as carbon nanotubes, metal nanoparticles and quantum dots are found in numerous industrial and consumer products [2].

In order to understand the fate and impact of ENP, it is critical to discriminate among the dissolved, nanoscale and bulk materials [3]. Of particular concern are ENPs that are released into municipal sewers from households, industrial sources, paints and coatings. Indeed, recent studies have predicted that significant loads of ENPs will accumulate in municipal wastewater treatment plants (WWTPs) [4, 5], resulting in levels of ENP, such as silver nanoparticles (Ag NP) [6] that may already pose risks to aquatic organisms [7, 8]. However, due to their low concentrations and the presence of a complex background matrix [4], few techniques are currently available for their detection [9]. Robust techniques that allow the quantification of ENP in wastewaters are only now beginning to emerge [5, 6, 10-12].

Hydrodynamic chromatography (HDC) [13, 14] can be used to separate ENP based upon their hydrodynamic diameters [15] (with the largest particles eluting first). Since it employs a column that limits interactions with the stationary phase, HDC has the potential to be a powerful, minimally perturbing technique for separating ENP in environmental samples [13]. By coupling HDC with inductively coupled plasma mass spectrometry (ICPMS), it is possible to attain the low concentrations that are expected to be found in natural samples [14]. By running the ICPMS in single particle detection mode (SP ICPMS; [16-18], particle size distributions can be obtained directly.

The goal of this study was to examine whether HDC could be used to identify and quantify ENP in a municipal wastewater sample. In order to evaluate the capacity of the technique, we first tested the hydrodynamic separation of several ENP standards (gold (nAu), polystyrene (nPS) and silver (Ag NP) nanoparticles) and their mixtures spiked into a municipal wastewater sample. Following the optimization of separation parameters (ENP concentration, eluent flow rate, etc.), the standard ENP were separated, detected and characterized, first at high concentrations (1-100 mg L^{-1}) using on-line light scattering detectors (static (SLS) and dynamic light scattering (DLS)) and then at environmentally relevant concentrations (1-20 µg L^{-1}) using inductively coupled plasma mass spectrometry (ICPMS) and single particle mode inductively coupled plasma mass spectrometry (SP ICPMS) [16, 19]. Using the optimized instrumental parameters, HDC ICPMS and HDC SP ICPMS were then performed on several spiked and unspiked wastewater and river water samples in order to determine the capacity of the technique to identify and quantify nanoparticles.

Materials and methods

Reagents. An optimized HDC eluent of 1 mM $NaNO_3$, 0.0013 % w/w SDS, 0.0013 % w/w Triton X-100 at a pH of 7.5 (±0.2) [10] was prepared using Milli-Q water (R > 18 MΩ cm, organic carbon < 2 µg L^{-1}); sodium nitrate (Fluka, >99%) to adjust the ionic strength and sodium hydroxide (Sigma-Aldrich, SigmaUltra) and nitric acid (Fluka, TraceSELECT®Ultra) to adjust the pH. Sodium dodecyl sulfate (SDS, G-Biosciences, Biotechnology grade) and Triton X-100 (Sigma Triton™X-100 BioUltra) were added to the eluent as anionic and non-ionic surfactants, respectively. pH measurements were made using a Metrohm 744 pH-meter. Sodium azide (0.02% w/w, Fisher Scientific) was added to eluent that was used to rinse the HDC column at the end of each experiment. A number of nanoparticle standards (polystyrene, gold and silver nanoparticles; Table 1) or their mixtures were used to validate the efficiency of the separations and optimize the separation parameters. A 100 mg L^{-1} solution of a fulvic acid (Suwannee River fulvic acid, SRFA; International Humic Substances Society, IS101F) was prepared for a limited number of injections on the HDC column.

Table 1. Standard nanoparticles employed for validation/optimization experiments. Nominal diameters were confirmed using a combination of dynamic light scattering (DLS), analytical ultracentrifugation and transmission electron microscopy.

ENP	Nominal diameter (nm)	Additional information
Polystyrene (nPS)	42.9, 51, 57, 60, 120	Bangs Laboratories Inc., 1% solids, NIST traceable particle size standards.
Gold (nAu)	60	Ted Pella Inc., PELCO® NanoXact™ tannic acid capped, pure ENP solution was 50 mg L^{-1}.
Gold (nAu)	60	NIST reference material, RM 8013, stock solution of 50 mg L^{-1}, citrate stabilized
Silver (Ag NP)	40, 80	Ted Pella Inc., PELCO® NanoXact™ citrate stabilized, pure ENP solution was 20 mg L^{-1}.

Hydrodynamic chromatography and on-line detection. A PL-PSDA, type 1 HDC column with a separation range of 5 to 300 nm, a length of 80 cm and an internal diameter of 7.5 mm (Agilent) was used on an Agilent 1260 Infinity Bio-inert quaternary HPLC fitted with an autosampler (Agilent 1260 Infinity Standard). Although this study was focused on the separation of nanoparticles in the 5-300 nm size range, HDC columns with other separation ranges are available. Particles that are larger than 300 nm are eluted at faster elution times, with little separation. All tubing was made of inert materials (mainly polytetrafluoroethylene), including the tubing used to connect the HDC column to the ICPMS. With the exception of the preliminary experiments, two optimized flow rates were employed, depending upon the detector: 0.50 mL min^{-1} (ICPMS) and 1.00 mL min^{-1} (light scattering detectors). An injection volume of 20 µL was employed with a pressure of approximately 3800 kPa for the eluent flow rate of 0.50 mL min^{-1} and a pressure of 7800 kPa at 1.00 mL min^{-1}. Both blanks and ENP standards were run frequently in order to monitor the analytical performance of the instruments. The detailed experimental protocol and justification

for some of the HDC separation parameters have been provided previously [13] and in the Supplementary Information (Tables S4-S6; Fig. S4).

A Dawn Heleos II detector (Wyatt Technologies) was employed for the acquisition of on-line static (SLS) and dynamic (DLS) light scattering data (scattering angle of 99°). Translational diffusion coefficients of the ENP were determined from the exponential decay of an autocorrelation function, which were then used to calculate hydrodynamic radii, R_h, based upon the Stokes-Einstein equation [20]. Where possible, the angular dependence of the scattered light (18 measured angles) was used to determine the particle's radius of gyration (R_g). For a spherical particle, R_g is related to its hydrodynamic radius by $R_g^2 = (3/5)\ R_h^2$. For the particles studied here (diameters of 40-120 nm), a linear order Zimm fit model was used to analyse the SLS data [21]. For some samples, particle diameters were also verified off-line, using a second DLS instrument (Mobius, Wyatt Technologies, scattering angle of 171.5°).

Data were also acquired by coupling an ICPMS (PerkinElmer NexION 300X) to the HDC column, using either classical or single particle (SP ICPMS). The following isotopes were used for quantification: ^{24}Mg, ^{26}Mg, ^{43}Ca, ^{60}Ni, ^{63}Cu, ^{66}Zn, ^{107}Ag, ^{197}Au. In classical ICPMS, elemental values are averaged over 3 s (integration time for a given isotope= 1 s, 3 replicates), whereas SP ICPMS uses the short-term (~ms) variations of the ICPMS signal to calculate nanoparticle concentrations and sizes. SP ICPMS experiments were carried out using the following data acquisition parameters: 1 sweep per read; 20,000 reads per replicate; settling time of 0.1 ms; dwell time of 100 µs (fast scan mode) and a flow rate of 0.50 mL min^{-1} (controlled by the HPLC pump). Nebulisation efficiency was determined from a NIST standard solution of nAu using the following parameters: sample flow rate (0.50 mL min^{-1}); concentration (100 ng L^{-1}); size (R_h = 30 nm); particle density (19320 kg m^{-3}) [22]. Particle number concentrations were determined from the frequency of detected pulses using the calculated nebulisation efficiency [23, 3]. For SP ICPMS of known ENP suspensions, concentrations were adjusted so that, statistically speaking, only single particles reached the mass spectrometer during any given measurement time (dwell time) [4]. For example, Ag NP concentrations ranging between 0.5 and 18 µg L^{-1} were injected into the HDC column in order to attain ENP concentrations that were in the range of 1 to 100 ng L^{-1} when they reached the mass spectrometer (dilution occurred mainly in the HDC column). A threshold limit of three standard deviations (3σ) above the background signal acquired using dissolved metal only was used to discriminate between dissolved metal and the ENP [4, 3, 24]. The minimal value of particle sizes that could be determined depended the intensity of the ENP signal with respect to that of the background for a given dwell time [22] (detection limits are provided below for a given set of experimental conditions). For ICPMS measurements, samples were acidified at the exit of the HDC column, whereas in SP ICPMS, samples were not acidified.

Sample collection and preparation. Experiments were performed with both spiked and unspiked samples. For the experiments involving Ag NP spikes, influent and effluent waters were collected from the Repentigny (Quebec, Canada) municipal treatment plant on February 21th 2014. Samples were pre-filtered through a 0.45 µm Nylon membrane (Millipore) in order to remove large aggregates and dust particles [25], prior to injection on the HDC column. HDC ICPMS and HDC SP

ICPMS experiments were always performed within 3 hours of Ag NP addition. For experiments without the nanoparticle spike, six additional samples were collected from three wastewater treatment plants and a local river (Table 2). These samples were also prefiltered prior to their injection on the HDC column. The prefiltration step was used to avoid potential problems associated with blockage and analysis with a concentric (rather than a high solids) nebulizer.

Table 2. Water sample identification. Detailed information on the content of the water samples is provided in Table S7.

Type of water	Date of sampling	Location of sampling	pH	Prefiltration
Influent	11-08-2014	Le Gardeur wastewater	7.18	0.45 µm
Effluent		treatment plant	7.12	0.45 µm
Effluent	20-03-2014	Montreal wastewater treatment plant	7.23	0.22 µm
Influent	05-09-2014	Repentigny wastewater	7.38	0.45 µm
Effluent		treatment plant	7.64	0.45 µm
River water	08-05-2014	Des Prairies river	7.37	0.22 µm

Means and standard deviations were determined from triplicate measurements. An analysis of variance was performed at $P = 0.05$ and where applicable, significant differences were identified using a Student-Newman-Keuls test or a Student t test, also at $P = 0.05$. Statistical tests were performed using standard deviations obtained from repeated measurements ($n = 3$) rather than the breadth of the particle size distributions. Although all separations were run in triplicate, only single representative chromatograms have been presented below. Mass balances were systematically performed in order to determine recoveries by comparing concentrations that were determined (ICPMS) with and without acidification and with and without separation (HDC). Non separated, acidified samples were used to determine 100% recovery. For samples separated by HDC, only concentrations collected between 23-30 minutes were used in the mass balance calculations.

Results and Discussion

Influence of experimental parameters on HDC performance. Numerous preliminary experiments were performed in order to evaluate the role of eluent flow rates and ENP concentrations on the resolution of multiple ENP peaks. When using light scattering detectors and mg L^{-1} concentrations of the ENP, the optimal resolution occurred at the highest tested flow rate of 1.50 mL min^{-1} (Figs. S1, S2; Tables S1, S2), whereas optimal separations for the HDC ICPMS/HDC SP ICPMS were obtained using a 0.50 mL min^{-1} flow rate (Fig. S3, Table S3). The calibration curve obtained at 0.5 mL min^{-1} for latex standards (nPS) is presented in Fig. 1.

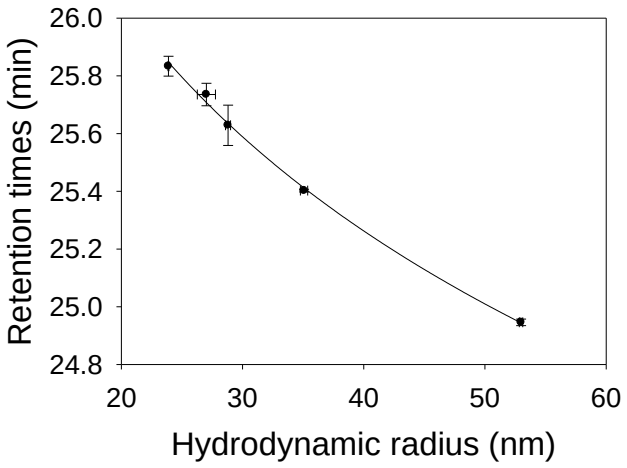

Fig. 1. Calibration curve obtained for latex particle standards at a flow rate of 0.50 mL min^{-1}. The curve (logarithmic fit, R^2 of 0.998) was obtained by plotting retention times as a function of the *measured* hydrodynamic radii obtained from light scattering (DLS).

Characterisation of the natural water samples (influents, effluents, river water). The main inorganic and organic components of the water samples were measured by ICPMS and an organic carbon analyser (Table S7). For the Repentigny station that was used for optimization, no major differences in the inorganic content of the influent and the effluent waters were observed, although, the influent water did contain substantially more organic carbon than the treated effluent. Particle size distributions of the Repentigny samples were determined using both off-line DLS and on-line HDC DLS/SLS. These results showed that the samples initially contained numerous particles in the nanoparticle size range with the potential capacity to mask signals from the ENP (Figure S5).

Standard ENP spiked into wastewater samples. Nanosilver (40 and 80 nm) was spiked into Milli-Q water or into the Repentigny samples (influent and effluent). When SP ICPMS was performed without prior separation by HDC (Table 3), extremely low particle concentrations were analysed (0.05 µg L^{-1} for the 40 nm Ag NP; 0.18 µg L^{-1} for the 80 nm Ag NP), corresponding to high particle recoveries (in Milli-Q water, 97% for the 40 nm Ag NP; 109% for the 80 nm Ag NP). Furthermore, in the Milli-Q water, particle sizes were consistent with the nominal sizes provided by the manufacturer (40 nm: 38.0 ± 0.4 nm; 80 nm: 76.2 ± 0.4 nm; Table 3). On the other hand, particle sizes measured by SP ICPMS were significantly (Student t-test, $P < 0.05$) smaller in the wastewaters (both influent and effluent) than those measured in the Milli-Q water. In addition, particle numbers appeared to decrease in both wastewaters when compared to Milli-Q water, although differences were not always significant given that there was a higher incertitude on particle number determinations in the complex matrices. Since no particle agglomeration was observed, SP ICPMS data suggested that the losses of Ag NP in the wastewater samples could mainly be attributed to particle dissolution. Indeed, concentrations of dissolved Ag measured by SP ICPMS were consistent with an important particle dissolution occurring in all three waters

(Table 3). Nonetheless, it should be noted that while agglomeration was not observed, heteroagglomeration of the Ag NP with natural colloids in the wastewaters was likely minimized by pre-filtering the samples prior to the addition of the spikes.

Table 3. SP ICPMS and HDC SP ICPMS measurements of two Ag NP (nominally 40, 80 nm) measured in Milli-Q water and the Repentigny influent and effluent. Nanoparticle concentrations were 100x greater when using HDC in order to account for sample dilution during elution. Particle diameters and concentrations are those determined by SP ICPMS at the maximum (Ag) peak intensities (± 0.2 min). Different letters in the superscripts means that for a given particle concentration, significant differences were obtained using a Student-Newman-Keuls test at P=0.05.

Ag NP	Analysis technique	Sample concentration (µg L^{-1})	Sample matrix	Diameter (nm)	Ag NP concentration (10^6 particles/L)	Dissolved concentration (µg L^{-1})	Retention time (min)
40 nm	SP ICPMS	0.05	Milli-Q water	38.0 ± 0.4^{a}	111 ± 6^{a}	0.056 ± 0.004	-
			Influent	32.6 ± 0.6^{a,b}	74 ± 27^{a,b}	0.070 ± 0.022	-
			Effluent	36.2 ± 2.8^{b}	85 ± 10^{b}	0.063 ± 0.008	-
	HDC SP ICPMS	5	Milli-Q water	40.8 ± 3.2^{a}	1272 ± 266^{a}	-	25.9 ± 0.3
			Influent	41.8 ± 2.8^{a}	905 ± 94^{a}	-	26.6 ± 1.4
			Effluent	38.0 ± 3.2^{a}	1015 ± 106^{a}	-	25.0 ± 0.5
80 nm	SP ICPMS	0.18	Milli-Q water	76.2 ± 0.4^{a}	87 ± 8^{a}	0.057 ± 0.005	-
			Influent	47.2 ± 11.9^{b}	58 ± 17^{a}	0.083 ± 0.026	-
			Effluent	71.0 ± 1.8^{c}	69 ± 10^{a}	0.065 ± 0.007	-
	HDC SP ICPMS	18	Milli-Q water	74.0 ± 5.0^{a}	1154 ± 377^{a}	-	25.4 ± 0.1
			Influent	61.4 ± 16.8^{a}	451 ± 90^{b}	-	25.1 ± 0.5
			Effluent	73.8 ± 17.6^{a}	814 ± 121^{a}	-	25.2 ± 1.0

When the HDC column was coupled to the SP ICPMS, retention times of 25.9 ± 0.3 min (40 nm) and 25.4 ± 0.1 min (80 nm) were found for the Ag NP in deionised water, in good agreement with the retention times that would be expected from the particle curve calibration (Fig. 1: 26.1 min for the 40 nm particles and 25.2 min for the 80 nm particles). Once again, both particle numbers and particle diameters appeared to decrease in the influent samples with respect to samples run in Milli-Q water. In the effluents, the observed decreases of ENP sizes and concentrations were not statistically significant (Table 3). For both influent and effluent samples, particle size distributions were broadened with respect to those obtained in Milli-Q water. Similar to the SP ICPMS measurements on the unfractionated samples, the observed reductions of particle numbers and particle sizes were consistent with a partial ENP dissolution and increased ENP polydispersity in the more complex sample matrices [26].

Due to their dilution during the chromatographic separation, samples that were injected onto the HDC column were initially 100x more concentrated than those measured directly by SP ICPMS; however, measured particle concentrations were only about ~10x greater (Table 3). The lower

than expected particle numbers resulted from the fact that only nanoparticles that had retention times between 23-30 minutes were considered in the quantification. In addition, some particle loss due to adsorption or capture of the Ag NP by the HDC column was likely to have occurred. Indeed, when the HDC was coupled to the ICPMS (i.e. classical mode using samples that were acidified post-column), Ag was detected in several ENP size fractions (Fig. 2), i.e. retention times from 23-30 minutes, although, concentrations were very near Ag detection limits (ca. 0.03 µg L^{-1}, Table S8). For the Milli-Q water samples (black lines, Fig. 2), most Ag was detected in the 25-26 minute interval, which corresponded to particle sizes of 20-50 nm. In the effluent samples (blue lines), retention times were displaced to longer retention times, corresponding to smaller particle sizes, for both Ag NP. A similar shift was observed for the 80 nm Ag NP in the influent but this was not the case for the smaller (40 nm) Ag NP where only a small peak was detected at 24.3 minutes, corresponding to a size of approximately 94.3 ± 0.4 nm (Fig. 1). Note that for both the influent and the effluent, Ag was observed in several Ag fractions, indicating either increased polydispersity of the Ag NP (due to their dissolution and/or agglomeration) or adsorption of Ag to colloidal particles in the samples.

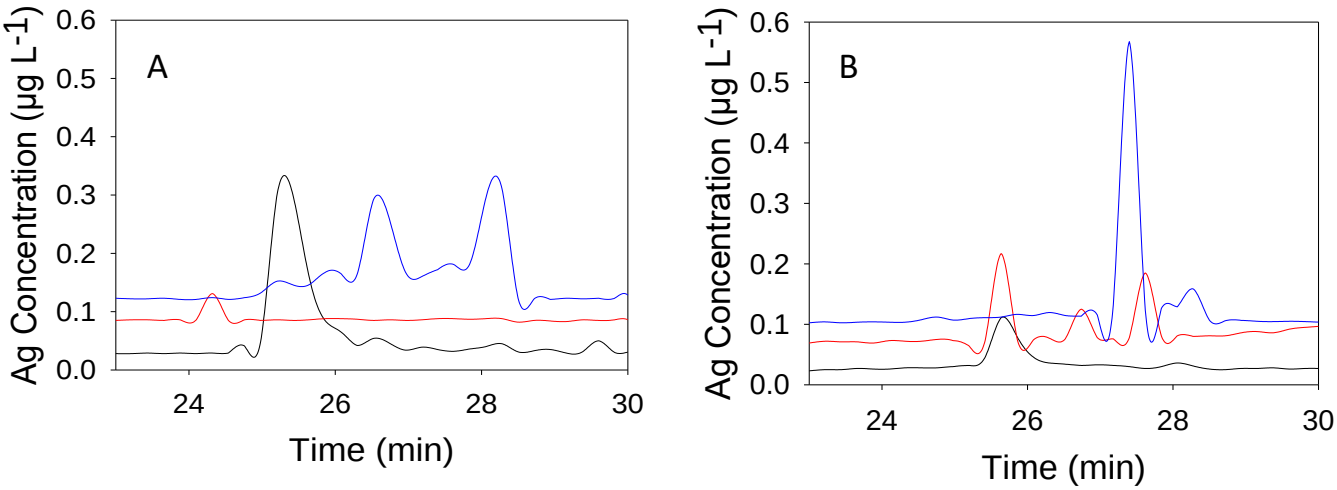

Fig. 2. HDC chromatograms generated from Ag concentrations from ICPMS (HDC ICPMS): (A) 40 nm Ag NP spiked at a concentration of 5 µg L^{-1} in Milli-Q water (black), WWTP influent (red) and WWTP effluent (blue line), and (B) 80 nm Ag NP spiked at a concentration of 18 µg L^{-1} in Milli-Q water (black), WWTP influent (red) and WWTP effluent (blue line). Note that the y-axis data for the influent and effluent samples have been shifted upwards by 0.05 and 0.1 µg L^{-1}, respectively, in order to facilitate identification of the chromatographic peaks. Samples were acidified post-column.

HDC chromatograms generated by SP ICPMS were consistent with those determined using ICPMS. For example, for the 80 nm Ag NP (Fig. 3), particles were detected with retention times between 24 and 28 min. The maximum signal intensity occurred at 25.2 minutes where a particle diameter of 73.8 nm was measured. A particle number detection limit of 26700 particles mL^{-1} (0.1 µg Ag L^{-1} for 80 nm particles) could be determined from 3x the standard deviation of the chromatographic

signal for retention times where no nanoparticles were expected (i.e. < 20 min; Fig. 3A). The HDC SP ICPMS detection limit of 0.1 μg Ag L^{-1} compares with a detection limit of 0.03 μg L^{-1} that could be determined in a similar manner from the HDC ICPMS results (Fig. 2). For the HDC SP ICPMS, due to the baseline variation, only particle diameters greater than 24 nm could be distinguished from their background signal as compared with the generally accepted minimum detectable diameter of 15 nm [22] that has been observed for a quadrupole ICPMS in single particle mode.

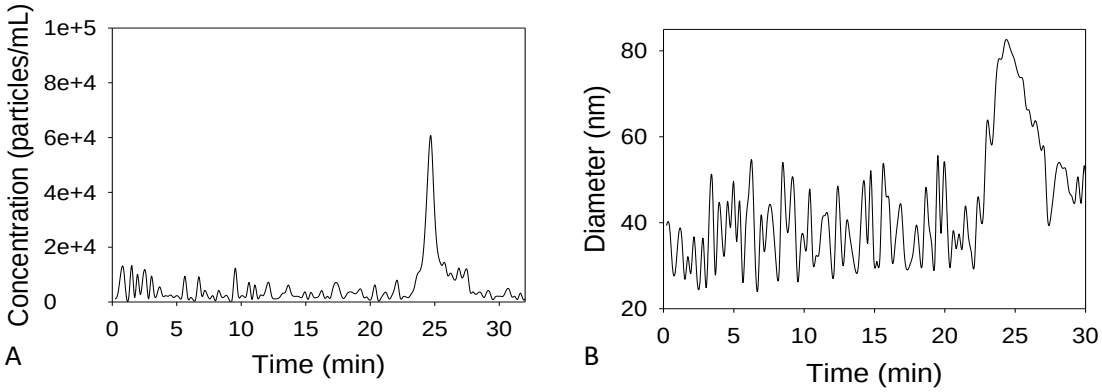

Fig. 3. HDC SP ICPMS chromatogram of the 80 nm Ag NP spiked into the Repentigny wastewater effluent at a concentration of 18 μg L^{-1}: (A) Ag NP particle concentrations and (B) Ag NP particle diameters (determined by SP ICPMS).

For chromatograms acquired using HDC SP ICPMS on the spiked samples, a much stronger signal was obtained for the Ag NP in deionised water (Fig. 4A, 4D) than for either the influent (4B, 4E) or effluent (4C, 4F) samples. Indeed, while peaks with the expected retention times were clearly visible in Milli-Q water, they were extremely difficult to distinguish from the baseline for the spiked influent samples. The nearly complete disappearance of peaks in the influent (Fig. 4B, 4E) was surprising, but could be explained both by a greater particle polydispersity; a greater proportion of nanoparticles that were below or near the (higher) detection limit for HDC SP ICPMS and by partial retention of the Ag by the HDC. Particle number concentrations decreased by 29% for the 40 nm Ag NP and by 61% for the 80 nm Ag NP. Since both HDC and SP ICPMS (but not ICPMS) are performed on non-acidified samples, it was expected that significant adsorptive losses could occur during those steps of the analysis. In fact, an average recovery of 103% was determined for the analysis of the Ag NP by SP ICPMS whereas losses of 50-90% were observed for HDC ICPMS (Table S8), suggesting that much of the decreased signal occurred due to adsorption of the Ag NP to the HDC column.

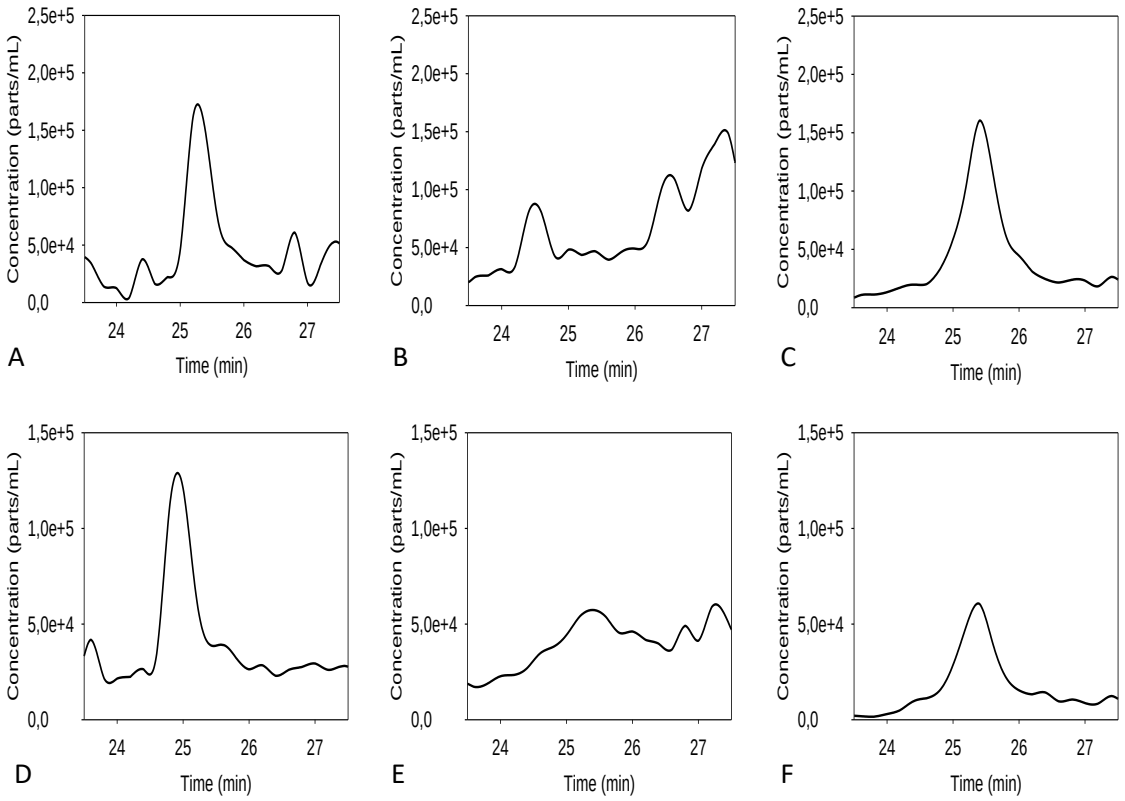

Fig. 4. HDC SP ICPMS chromatograms for 5 µg L^{-1} of 40 nm Ag NP spiked into (A) Milli-Q water, (B) wastewater influent and (C) wastewater effluent and for 18 µg L^{-1} of 80 nm Ag NP spiked into (D) Milli-Q water, (E) wastewater influent and (F) wastewater effluent.

ENP mixtures spiked into wastewater samples. A mixture of the two Ag NP was spiked into the three waters and then separated by HDC SP ICPMS. Once again, in the influent waters (Fig. 5B), it was difficult to resolve the Ag NP from the baseline. In that case, only a single peak corresponding to 45.6 ± 1.8 nm could be detected. In Milli-Q water (Fig. 5A) and in the effluent (Fig. 5C), peaks corresponding to the two Ag NP could be partially resolved. For the mixture in Milli-Q water, a diameter of 76.0 ± 5.8 nm was determined at the maximum intensity for the first peak (nominal size of 80 nm) whereas a diameter of 50.8 ± 3.0 nm was evaluated for the second peak (nominally 40 nm). In the effluent, a measured diameter of 71.4 ± 5.6 nm was determined for the 80 nm Ag NP whereas a value of 52.0 ± 5.4 nm was measured for the 40 nm Ag NP.

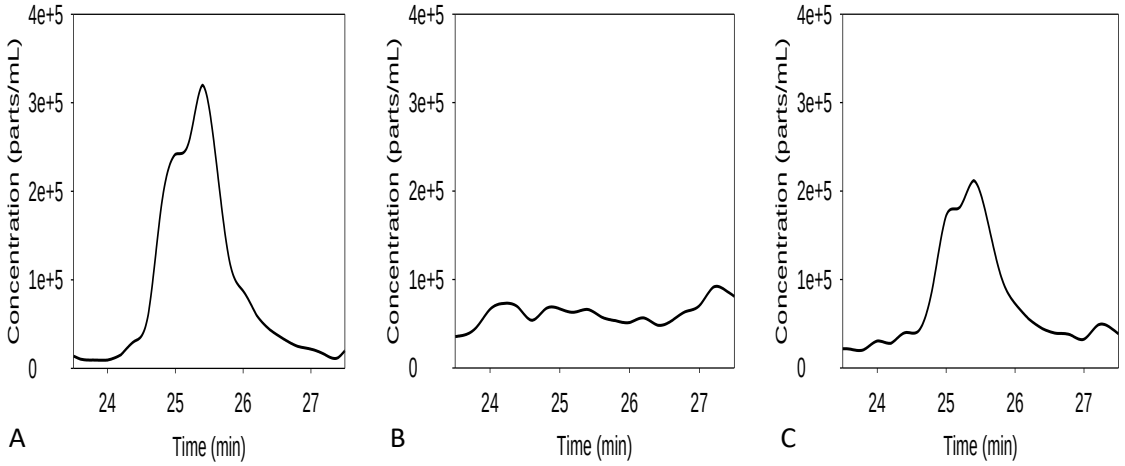

Fig. 5. HDC SP ICPMS chromatograms of a Ag NP mixture containing 5 µg L^{-1} of a 40 nm Ag NP and 18 µg L^{-1} of an 80 nm Ag NP spiked into (A) Milli-Q water, (B) influent water and (C) effluent water.

Above, hydrodynamic chromatography was coupled to the ICPMS, either in standard mode or in single particle detection (SP ICPMS). The optimized technique and knowledge of the method detection limits were subsequently employed to examine several non-spiked waters that were collected from three WWTP and a river (Table 2).

Characterisation of non-spiked samples. Influent, effluent and river water samples were analysed by using the HDC ICPMS and the HDC SP ICPMS, with an emphasis on detecting Ag NP. For all samples, Ag NP and dissolved Ag were below at least one of the HDC SP ICPMS detection limits (26700 particles L^{-1}; ca. 0.1 µg L^{-1} ; particle size of 24 nm). When HDC ICPMS was used (detected elements: Ag, Ca, Cu, Ni, Zn and Mg), only Cu nanoparticles (Cu NP, detection limit of 0.1 µg L^{-1}) were identified in the samples (Fig. 6). Nanosilver (Ag detection limit of 0.03 µg L^{-1}) while other potential NP (containing Ca, Cu, Ni, Zn, Mg) were below detection limits (Table 4). Note that the retention times for the Cu NP were high (mean of 28.4 ± 0.5 min), which corresponded to a particle size of approximately 2.5 nm (Fig. 1). Such sizes are highly suggestive of colloidal humic substances. Indeed, when 100 mg L^{-1} of a fulvic acid standard (SRFA) was spiked with Cu (Fig. S6), very similar retention times (28.8 ± 0.2 min) with respect to those observed in the non-spiked water samples were obtained. Interestingly, effluent samples had lower concentrations of the Cu NP than their corresponding influents.

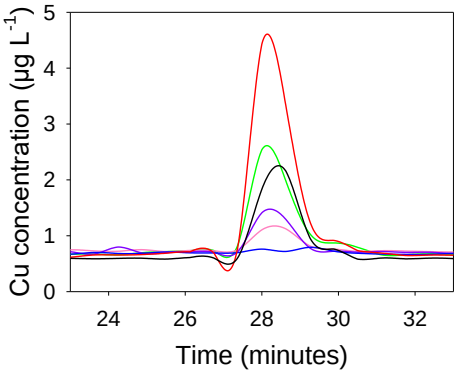

Fig. 6. HDC ICPMS chromatograms of the non-spiked water samples using ICPMS detection for Cu (from largest to smallest peaks): influent sample from Repentigny WWTP (red); influent sample of *Le Gardeur* WWTP (green); effluent sample from Repentigny WWTP (black); effluent sample from Montreal WWTP (purple), effluent sample of *Le Gardeur* WWTP (pink); freshwater from *Des Prairies* River (blue line).

Table 4. Detection limits of selected elements analysed by HDC ICPMS.

Elements	Detection limits ($\mu g\ L^{-1}$)
Mg	3.6
Ca	3.2
Ni	0.04
Cu	0.10
Zn	0.03
Ag	0.03

Recommendations. Overall, it was difficult to identify ENP in the complex environmental matrices such as wastewater influents and effluents using either of the complementary techniques (HDC ICPMS; HDC SP ICPMS). While the HDC separated the nanomaterials as a function of their hydrodynamic sizes (largest to smallest), thus providing some additional information on particle sizes from the retention times, it also resulted in an important sample dilution. The use of the type 1 HDC column and the ICPMS as a detector set an effective upper limit of 300 nm with respect to the particles that could be resolved, although other columns (e.g. type 2 HDC, 20-1200 nm) and other detectors (e.g. light scattering) would not have those same limitations. While dilution was generally not a problem when the ICPMS was employed with acidified samples, confirmatory information on particle sizes and numbers was often lost, as compared to SP ICPMS mode. Nonetheless, HDC SP ICPMS was able to detect particle dissolution in the natural samples (leading to lower (detected) particle numbers). When the optimized technique was employed to detect NP in several WW samples, nanoparticles were generally below method detection limits (i.e. Ag NP size limit of 24 nm; 26700 particles mL^{-1}; Ag concentration limit of 0.1 $\mu g\ L^{-1}$), however, small (ca. 2.5 nm) Cu NP were detected in the non-spiked WW samples. When using real samples, HDC

has the advantage of separating and diluting complex, particle containing matrices, thus potentially increasing the signal to noise, especially when using specific detectors like the ICPMS (in SP mode or not). While the coupling of HDC with ICPMS and SP ICPMS will certainly require further exploration and optimisation, the coupling of less-diluting separation techniques such as field flow fractionation [27, 28] or the use of ion exchange resins [29] may be even more promising route to reducing the matrix effects associated with the analysis of complex samples by SP ICPMS.

Acknowledgments

Funding for this work was provided by the Natural Sciences and Engineering Research Council of Canada, the *Fonds de Recherche du Québec - Nature et Technologies*, the Canadian Water Network and the City of Calgary. Assistance from the Repentigny, *Le Gardeur* and Montreal WWTP and the groups of Y. Comeau (*École Polytechnique*) and S. Ghoshal (McGill) was also greatly appreciated.

Conflicts of Interest

The authors declare having no conflicts of interest related to this publication.

References

1. Hochella MF. Nanoscience and technology the next revolution in the Earth sciences. Earth and Planetary Science Letters. 2002;203(2):593-605. doi:10.1016/s0012-821x(02)00818-x.
2. Rejeski D, T. Kuiken, and E. Pauwels. Project on Emerging Nanotechnologies. 2013. http;//www.nanotechproject.org/.
3. Pace HE, Rogers NJ, Jarolimek C, Coleman VA, Gray EP, Higgins CP et al. Single Particle Inductively Coupled Plasma-Mass Spectrometry: A Performance Evaluation and Method Comparison in the Determination of Nanoparticle Size. Environmental Science & Technology. 2012;46(22):12272-80. doi:10.1021/es301787d.
4. Mitrano DM, Lesher EK, Bednar A, Monserud J, Higgins CP, Ranville JF. Detecting nanoparticulate silver using single-particle inductively coupled plasma-mass spectrometry. Environmental Toxicology and Chemistry. 2012;31(1):115-21. doi:10.1002/etc.719.
5. Pycke BFG, Benn TM, Herckes P, Westerhoff P, Halden RU. Strategies for quantifying C-60 fullerenes in environmental and biological samples and implications for studies in environmental health and ecotoxicology. Trac-Trends in Analytical Chemistry. 2011;30(1):44-57. doi:10.1016/j.trac.2010.08.005.
6. Gottschalk F, Ort C, Scholz RW, Nowack B. Engineered nanomaterials in rivers - Exposure scenarios for Switzerland at high spatial and temporal resolution. Environmental Pollution. 2011;159(12):3439-45. doi:10.1016/j.envpol.2011.08.023.
7. Mueller NC, Nowack B. Exposure modeling of engineered nanoparticles in the environment. Environmental Science & Technology. 2008;42(12):4447-53. doi:10.1021/es7029637.
8. Schultz AG, Boyle D, Chamot D, Ong KJ, Wilkinson KJ, McGeer JC et al. Aquatic toxicity of manufactured nanomaterials: challenges and recommendations for future toxicity testing. Environmental Chemistry. 2014;11(3):207-26. doi:10.1071/en13221.
9. Mitrano DM, Barber A, Bednar A, Westerhoff P, Higgins CP, Ranville JF. Silver nanoparticle characterization using single particle ICP-MS (SP-ICP-MS) and asymmetrical flow field flow

363 fractionation ICP-MS (AF4-ICP-MS) (vol 27, pg 1131, 2012). Journal of Analytical Atomic
364 Spectrometry. 2013;28(12):1949-.
365 10. Tiede K, Boxall ABA, Wang X, Gore D, Tiede D, Baxter M et al. Application of hydrodynamic
366 chromatography-ICP-MS to investigate the fate of silver nanoparticles in activated sludge.
367 Journal of Analytical Atomic Spectrometry. 2010;25(7):1149-54. doi:10.1039/b926029c.
368 11. von der Kammer F, Ferguson PL, Holden PA, Masion A, Rogers KR, Klaine SJ et al. Analysis of
369 engineered nanomaterials in complex matrices (environment and biota): General considerations
370 and conceptual case studies. Environmental Toxicology and Chemistry. 2012;31(1):32-49.
371 doi:10.1002/etc.723.
372 12. Weinberg H, Galyean A, Leopold M. Evaluating engineered nanoparticles in natural waters.
373 Trac-Trends in Analytical Chemistry. 2011;30(1):72-83. doi:10.1016/j.trac.2010.09.006.
374 13. Proulx K, Wilkinson KJ. Separation, detection and characterisation of engineered
375 nanoparticles in natural waters using hydrodynamic chromatography and multi-method
376 detection (light scattering, analytical ultracentrifugation and single particle ICP-MS).
377 Environmental Chemistry. 2014;11(4):392-401. doi:10.1071/en13232.
378 14. Philippe A, Schaumann GE. Evaluation of Hydrodynamic Chromatography Coupled with UV-
379 Visible, Fluorescence and Inductively Coupled Plasma Mass Spectrometry Detectors for Sizing
380 and Quantifying Colloids in Environmental Media. Plos One. 2014;9(2).
381 doi:10.1371/journal.pone.0090559.
382 15. Striegel AM, Brewer AK. Hydrodynamic Chromatography. In: Cooks RG, Yeung ES, editors.
383 Annual Review of Analytical Chemistry, Vol 5. Annual Review of Analytical Chemistry, 2012. p.
384 15-34.
385 16. Degueldre C, Favarger PY. Colloid analysis by single particle inductively coupled plasma-mass
386 spectroscopy: a feasibility study. Colloid Surface A. 2003;217(1-3):137-42. doi:10.1016/s0927-
387 7757(02)00568-x.
388 17. Degueldre C, Favarger PY, Wold S. Gold colloid analysis by inductively coupled plasma-mass
389 spectrometry in a single particle mode. Analytica Chimica Acta. 2006;555(2):263-8.
390 doi:10.1016/j.aca.2005.09.021.
391 18. Rakcheev D, Philippe A, Schaumann GE. Hydrodynamic Chromatography Coupled with Single
392 Particle-Inductively Coupled Plasma Mass Spectrometry for Investigating Nanoparticles
393 Agglomerates. Analytical Chemistry. 2013;85(22):10643-7. doi:10.1021/ac4019395.
394 19. Laborda F, Jimenez-Lamana J, Bolea E, Castillo JR. Selective identification, characterization
395 and determination of dissolved silver(I) and silver nanoparticles based on single particle
396 detection by inductively coupled plasma mass spectrometry. Journal of Analytical Atomic
397 Spectrometry. 2011;26(7):1362-71. doi:10.1039/c0ja00098a.
398 20. Chen M. Introduction to Dynamic light Scattering and Phase Analysis Light Scattering. Wyatt
399 Technology Corporation: Santa Barbara, California. 2013.
400 21. Larkin M. Introduction to Light Scattering and Phase Analysis Light Scattering. Wyatt
401 Technology Corporation: Santa Barbara, California. 2013.
402 22. Hadioui M, Peyrot C, Wilkinson KJ. Improvements to Single Particle ICPMS by the Online
403 Coupling of Ion Exchange Resins. Anal Chem. 2014;86(10):4668-74. doi:10.1021/ac5004932.
404 23. Pace HE, Rogers NJ, Jarolimek C, Coleman VA, Higgins CP, Ranville JF. Determining Transport
405 Efficiency for the Purpose of Counting and Sizing Nanoparticles via Single Particle Inductively
406 Coupled Plasma Mass Spectrometry. Analytical Chemistry. 2011;83(24):9361-9.
407 doi:10.1021/ac201952t.
408 24. Franze B, Strenge I, Engelhard C. Single particle inductively coupled plasma mass
409 spectrometry: evaluation of three different pneumatic and piezo-based sample introduction

systems for the characterization of silver nanoparticles. Journal of Analytical Atomic Spectrometry. 2012;27(7):1074-83. doi:10.1039/c2ja00003b.
25. Cumberland SA, Lead JR. Particle size distributions of silver nanoparticles at environmentally relevant conditions. Journal of Chromatography A. 2009;1216(52):9099-105. doi:10.1016/j.chroma.2009.07.021.
26. Rakcheev DP, A.; Schaumann, G. E. Hydrodynamic chromatography coupled with single particle-inductively coupled plasma mass spectrometry for investigating nanoparticles agglomerates. Anal Chem. 2013;85:10643-7.
27. Meermann B. Field-flow fractionation coupled to ICP-MS: separation at the nanoscale, previous and recent application trends. Analytical and Bioanalytical Chemistry. 2015;407(10):2665-74. doi:10.1007/s00216-014-8416-1.
28. Meisterjahn B, Neubauer E, Von der Kammer F, Hennecke D, Hofmann T. Asymmetrical flow-field-flow fractionation coupled with inductively coupled plasma mass spectrometry for the analysis of gold nanoparticles in the presence of natural nanoparticles. Journal of Chromatography A. 2014;1372:204-11. doi:10.1016/j.chroma.2014.10.093.
29. Hadioui M, Merdzan V, Wilkinson KJ. Detection and Characterization of ZnO Nanoparticles in Surface and Waste Waters Using Single Particle ICPMS. Environmental science & technology. 2015;49(10):6141-8. doi:10.1021/acs.est.5b00681.